



**University of  
Zurich**<sup>UZH</sup>

**Zurich Open Repository and  
Archive**

University of Zurich  
Main Library  
Strickhofstrasse 39  
CH-8057 Zurich  
[www.zora.uzh.ch](http://www.zora.uzh.ch)

---

Year: 2012

---

## **Absolute value and anisotropy of the magnetic penetration depth in YBa<sub>2</sub>Cu<sub>3</sub>O<sub>6.92</sub>**

Hossain, M D; Baglo, J C; Wojek, B M; Ofer, O; Dunsiger, S R; Morris, G D; Prokscha, T; Saadaoui, H; Salman, Z; Bonn, D A; Liang, R; Hardy, W N; Suter, A; Morenzoni, E; Kiefl, R F

**Abstract:** The absolute value and anisotropy of the magnetic penetration depth have been measured in a mosaic of optimally-doped YBa<sub>2</sub>Cu<sub>3</sub>O<sub>6.92</sub> crystals using low-energy muon spin rotation at 8 K with extrapolation to  $T = 0$  using microwave resonator data. The average magnetic field was measured as a function of muon implantation energy in a small magnetic field applied along the  $\hat{a}$  and  $\hat{c}$  directions. Beyond a depth  $d$ , the magnetic field profiles are consistent with the simple exponential decay of the internal field expected from a London model. The results are compared with other less direct methods.

DOI: 10.1016/j.phpro.2012.04.081

Posted at the Zurich Open Repository and Archive, University of Zurich

ZORA URL: <http://doi.org/10.5167/uzh-64410>

Accepted Version

Originally published at:

Hossain, M D; Baglo, J C; Wojek, B M; Ofer, O; Dunsiger, S R; Morris, G D; Prokscha, T; Saadaoui, H; Salman, Z; Bonn, D A; Liang, R; Hardy, W N; Suter, A; Morenzoni, E; Kiefl, R F (2012). Absolute value and anisotropy of the magnetic penetration depth in YBa<sub>2</sub>Cu<sub>3</sub>O<sub>6.92</sub>. *Physics Procedia*, 30:235-240.

DOI: 10.1016/j.phpro.2012.04.081

# Absolute Value and Anisotropy of the Magnetic Penetration Depth in $\text{YBa}_2\text{Cu}_3\text{O}_{6.92}$

M. D. Hossain,<sup>1,2,\*</sup> J. C. Baglo,<sup>1</sup> B. M. Wojek,<sup>3,4</sup> Oren Ofer,<sup>2</sup> S. R. Dunsiger,<sup>5</sup>  
G. D. Morris,<sup>2</sup> T. Prokscha,<sup>3</sup> H. Saadaoui,<sup>3</sup> Z. Salman,<sup>3</sup> D. A. Bonn,<sup>1,6</sup> Ruixing  
Liang,<sup>1,6</sup> W. N. Hardy,<sup>1,6</sup> A. Suter,<sup>3</sup> E. Morenzoni,<sup>3</sup> and R. F. Kiefl<sup>1,2,6</sup>

<sup>1</sup>*Department of Physics and Astronomy, University of British Columbia, Vancouver, BC, Canada V6T 1Z1*

<sup>2</sup>*TRIUMF, 4004 Wesbrook Mall, Vancouver, BC, Canada V6T 2A3*

<sup>3</sup>*Laboratory for Muon-Spin Spectroscopy, Paul Scherrer Institute, 5232 Villigen PSI, Switzerland*

<sup>4</sup>*Physik-Institut, Universität Zürich, 8057 Zürich, Switzerland*

<sup>5</sup>*Physik Department E21, Technische Universität München, 85748 Garching, Germany*

<sup>6</sup>*Canadian Institute for Advanced Research, Toronto, Ontario, Canada M5G 1Z8*

The absolute value and anisotropy of the magnetic penetration depth have been measured in a mosaic of optimally doped  $\text{YBa}_2\text{Cu}_3\text{O}_{6.92}$  crystals using low-energy muon-spin rotation at 8 K with extrapolation to  $T = 0$  using microwave resonator data. The average magnetic field was measured as a function of muon implantation energy in a small magnetic field applied along the  $\hat{a}$  and  $\hat{b}$  directions. Beyond a depth  $d$ , the magnetic field profiles are consistent with the simple exponential decay of the internal field expected from a London model. The results are compared with other less direct methods.

## INTRODUCTION

One of the most important observables in any superconductor is the London penetration depth  $\lambda$ , since it is closely related to superfluid density ( $\rho_s \propto 1/\lambda^2$ ) and the magnitude of the order parameter. Measurements of the absolute value of  $\lambda$  and its variation as a function of temperature, magnetic field, crystal orientation, and doping are important tests of theories of unconventional superconductivity. For example, the approximate linear correlation between  $\rho_s$  and  $T_c$  in many exotic superconductors has stimulated considerable discussion about the nature of high- $T_c$  superconductivity [1]. Most of these measurements were carried out with bulk TF (transverse field)  $\mu\text{SR}$  (muon-spin rotation) on powders where there is considerable uncertainty in the absolute value of  $\lambda$  due to the high degree of vortex-lattice disorder. Measurements on single crystals of  $\text{YBa}_2\text{Cu}_3\text{O}_{6+x}$  both in the Meissner [2, 3] and vortex phases [2] have found that  $1/\lambda^2$  is a sublinear function of  $T_c$ . This can be understood in terms of a three-dimensional quantum critical point (QCP) model [4]. An additional complexity in compounds such as  $\text{YBa}_2\text{Cu}_3\text{O}_{6+x}$  and  $\text{YBa}_2\text{Cu}_4\text{O}_8$  is that they have one-dimensional  $\text{CuO}$  chains in close proximity to the  $\text{CuO}_2$  planes. Such chains will exert a potential on charged currents moving in the  $\text{CuO}_2$  planes, which should lead to an  $a$ - $b$  anisotropy in the magnetic penetration depth. It is also possible that well ordered chains contribute directly to the condensate which would alter the relationship between  $T_c$  and  $\rho_s$ . A recent study in  $\text{YBa}_2\text{Cu}_4\text{O}_8$  reports the  $a$ - $b$  anisotropy in  $\Delta\lambda$  is a strong function of temperature and magnetic field [5]. One explanation is that the planes and chains are coupled via a proximity effect which is weakened at higher temperatures and magnetic fields. It is clear that accurate measurements of  $\lambda_a$  and  $\lambda_b$  may help clarify some central issues in  $\text{YBa}_2\text{Cu}_3\text{O}_{6+x}$  and its relationship to other su-

perconductors.

In this paper we report a direct measurement of magnetic penetration in the Meissner state on a small mosaic of oriented optimally-doped  $\text{YBa}_2\text{Cu}_3\text{O}_{6.92}$  single crystals at 8 K using low-energy  $\mu\text{SR}$ . This is the most direct method for measuring the magnetic penetration depth in a superconductor [6] but until recently it has been restricted to studies on large area samples. The current work extends the use of low energy  $\mu\text{SR}$  to crystals which are smaller than the beam spot [7]. The field profiles were measured with a small magnetic field applied parallel to either the  $\hat{a}$  or  $\hat{b}$  axis at  $T = 8$  K, and the fitted values for  $\lambda$  were then extrapolated to  $T = 0$  using microwave resonator data. The results are compared with other less direct methods.

## EXPERIMENTAL

The experiment was performed at the  $\mu\text{E4}$  hybrid-type beam line at the Paul Scherrer Institute (PSI, Switzerland), which produces an intense beam ( $10^4/\text{s}$ ) of polarized  $\mu^+$  using a solid Ar moderator capped with  $\text{N}_2$ . Muons leaving the moderator have an average energy of 20 eV and are subsequently accelerated to 15 keV and transported electrostatically to the  $\mu\text{SR}$  spectrometer  $\sim 2.2$  m away. The spectrometer and transport system are maintained in ultra high vacuum at all times. A carbon foil trigger detector is used to detect incoming muons, which reach the entrance of the cryostat with a mean energy of 14.1 keV and an asymmetric energy spread of 0.42 keV. The muon implantation energy is controlled by applying an electrostatic potential to the sample holder which is separated from the cryostat by a sapphire plate. Further details on low energy muon production, the  $\mu\text{E4}$  beamline and the spectrometer may be found in Refs. 8 and 9.

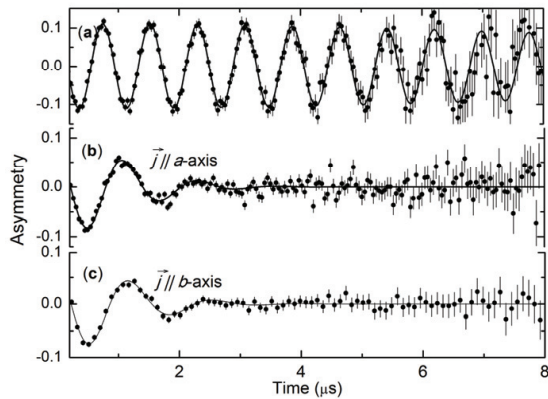


FIG. 1. (a) The muon-spin-precession signal in the normal state of  $\text{YBa}_2\text{Cu}_3\text{O}_{6.92}$  at 110 K in an external field of 9.46 mT applied parallel to the  $\hat{a}$  direction. (b) The same conditions as (a) except in the superconducting state at  $T = 8$  K with the external magnetic field along the  $\hat{b}$  direction. (c) The same as (b) except the field is along the  $\hat{a}$  direction.

A key aspect of the current experiment, which allows the study of small crystals without interference from a background signal, is that the sample holder is coated with 1  $\mu\text{m}$  of ferromagnetic Ni. Consequently, muons that miss the sample experience large hyperfine fields [10], lose polarization very quickly, and are thus removed from the frequency range of interest. The geometry is such that the thin Ni layer does not perturb the magnetic field seen by muons in the sample. Each of the  $\text{YBa}_2\text{Cu}_3\text{O}_{6.92}$  crystals was approximately rectangular in shape, with lateral dimensions in the  $a$ - $b$  plane ranging from (1 to 3) mm and a thickness in the  $\hat{c}$  direction ranging from (0.1 to 0.3) mm. They were detwinned to a level greater than 95 % and covered a total area of 55  $\text{mm}^2$ .

## RESULTS

Figure 1a shows the measured muon precession signal in the normal state of the  $\text{YBa}_2\text{Cu}_3\text{O}_{6.92}$  mosaic in a small external magnetic field (9.46 mT) applied parallel to the surface. Meissner screening below  $T_c$  is evident from the reduced precession frequency for both orientations, as shown in Figs. 1b and 1c. The signals were fit according to the following procedure. At any given implantation energy, the stopping distribution  $\rho(z)$  was calculated using the TRIM.SP ion implantation code [11], whose accuracy has been tested in previous experiments [12]. The magnetic field profile in the Meissner state was assumed to be of the form:

$$B(z) = \begin{cases} B_0 \exp[-(z-d)/\lambda_{a,b}] & z \geq d \\ B_0 & z < d \end{cases}, \quad (1)$$

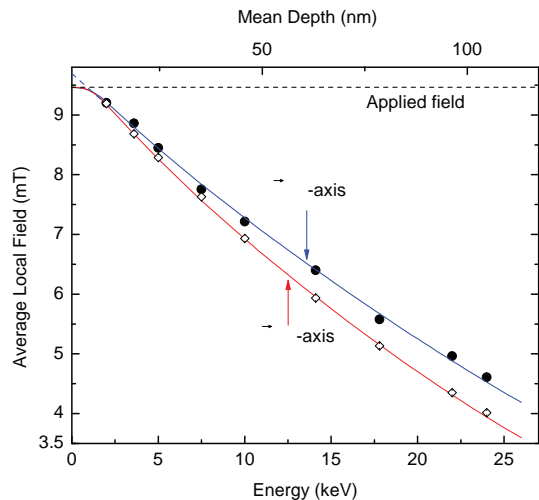


FIG. 2. The average magnetic field versus mean stopping depth in an applied field of 9.46 mT when the shielding currents are flowing in the  $\hat{a}$  direction ( $\vec{j} \parallel \hat{a}$ , filled circles) and  $\hat{b}$  direction ( $\vec{j} \parallel \hat{b}$ , open diamonds). The curves are the average fields generated from a global fit of all the spectra at 8 K taken at all energies and for both orientations. The common parameters are  $\lambda_a$ ,  $\lambda_b$  and  $d$ . The individual points are from a fit to the same model but at individual implantation energies.

where  $B_0$  is the magnitude of the applied field,  $\lambda_{a,b}$  is the magnetic penetration depth with the magnetic field applied parallel to the  $\hat{a}$  or  $\hat{b}$  axis respectively,  $z$  is the depth into the crystal, and  $d$  is an effective dead layer within which the supercurrent density is suppressed. A theoretical muon precession signal  $\mathcal{A}(t)$  was then generated by averaging over the calculated stopping distribution  $\rho(z)$ :

$$\mathcal{A}(t) = A \exp[-\sigma^2 t^2 / 2] \int \rho(z) \cos[\gamma_\mu B(z)t + \phi] dz, \quad (2)$$

where  $\gamma_\mu$  is the muon gyromagnetic ratio,  $A$  is the initial amplitude of precession,  $\phi$  is the initial phase of the incoming muon spins, and  $\sigma$  is a parameter which reflects any inhomogeneous broadening. For the energy scans  $\phi$ ,  $d$ ,  $\lambda_a$  and  $\lambda_b$  are treated as global fit parameters.

Figure 2 shows the average local field [ $\langle B \rangle = \int \rho(z) B(z) dz$ ] determined from single-energy fits as a function of muon implantation energy (bottom scale) and the corresponding mean implantation depth (top scale). The filled circles and open diamonds are from data taken with the shielding currents flowing along the  $\hat{a}$  and  $\hat{b}$  axes respectively (or equivalently the magnetic field along the  $\hat{b}$  and  $\hat{a}$  axes). The corresponding curves are generated from a global fit of runs taken at 8 K for both orientations and all energies; a comparison between the data points and curves reflects how closely the data at each energy agrees with the global fit. The best fit yields  $\lambda_a = 131.4(5)$  nm,  $\lambda_b = 109.8(5)$  nm, and  $d = 9.1(2)$  nm,

where the uncertainties given are purely statistical. Our model provides an excellent fit to the data as indicated by the fact that the  $\chi^2$  per degree of freedom is 1.07. However, there are sources of potential systematic uncertainty; for example, there is uncertainty in the implantation profiles calculated with TRIM.SP, corresponding to a 3 % uncertainty in the mean depth, which translates into similar errors in  $\lambda_a$  and  $\lambda_b$ . In addition, the fitted  $\phi$  from the global fit or in free phase fits is about  $9^\circ$  higher than in the normal state. Extensive simulations of the experiment were unable to account for a phase shift this large [13]. One possibility is that the TRIM.SP stopping distributions and resulting frequency distributions are more asymmetric than predicted. Finally, the assumed field profile has a dead layer whose origin is still unclear. Recent simulations confirm that surface roughness on the scale of  $d$  could partially account for the deviation from a perfect London model profile [14]. Also some suppression of the supercurrent density is expected as a result of the discontinuous nature of electronic properties near a surface, although one would expect the order parameter to reach the bulk value on a length scale much shorter than  $d$ . We note that this apparent dead layer, although taken into account in the current measurement, may have important consequences since the same effect could influence any Meissner state measurement of  $\lambda$  and to some extent its temperature dependence. For example, any small temperature dependence in  $d$  would influence precision measurements of  $\Delta\lambda$  obtained from microwave resonator or tunnel diode resonator techniques. Additional experiments will be needed to investigate how  $d$  depends on temperature and magnetic field.

The absolute values of  $\lambda_a$  and  $\lambda_b$  were extrapolated to  $T = 0$  (as shown in Fig. 3) using  $\Delta\lambda$  measurements made using a microwave resonance technique. Microwave resonance provides a very precise measure of the temperature dependence of  $\lambda$  but is insensitive to its absolute value. Combining both methods is thus a very powerful way to investigate variations in the superfluid density. Microwave penetration depth measurements were obtained using a 942 MHz Nb loop-gap resonator operated as an oscillator (described previously in Ref. 15). A detwinned  $5.8 \mu\text{m}$ -thick platelet of  $\text{YBa}_2\text{Cu}_3\text{O}_{6.92}$  was mounted with a small amount of vacuum grease to a sapphire plate hot finger, loaded into the loop-gap cavity such that the microwave fields are applied parallel to the  $a$ - $b$  plane. Measurements of relative changes  $\Delta\lambda(T)$  in the penetration depth as a function of temperature were taken from (1.5 to 105) K for both the  $\hat{a}$  and  $\hat{b}$  directions with sub-ångström resolution; corrections have been applied for thermal expansion, thin-limit effects, and  $\hat{c}$ -axis contributions, as well as for remnant twinning. Combining this microwave data with the low-energy  $\mu\text{SR}$  data, our extrapolated values for the  $T = 0$  penetration depths, including systematic uncertainties, are  $\lambda_a(0) = 128.2(3.0)$  nm,  $\lambda_b(0) = 106.5(3.1)$  nm with

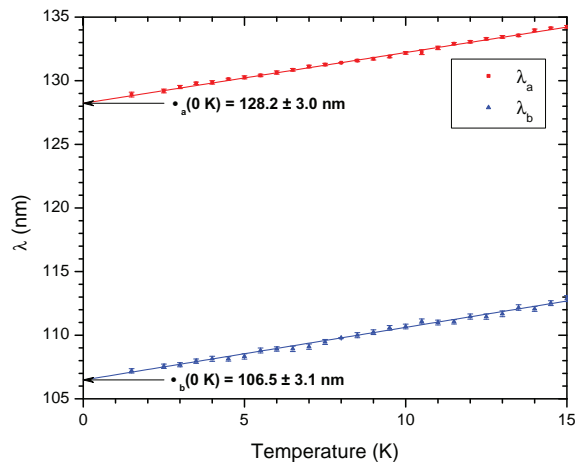


FIG. 3. Temperature dependence of the magnetic penetration depth in an external magnetic field applied parallel to the  $\hat{a}$  and  $\hat{b}$  axes, obtained by combining microwave resonator data with low-energy  $\mu\text{SR}$ . Absolute values of  $\lambda$  are obtained from low-energy  $\mu\text{SR}$  at 8 K given in the text, whereas  $\Delta\lambda(T)$  data are from microwave resonator measurements. The observed linear temperature dependence is consistent with that expected for a  $d$ -wave superconductor.

a ratio  $\lambda_a/\lambda_b = 1.20(1)$ . The values reported here are slightly different than in Ref. 7 due to an improved fitting procedure in which the phase is treated as global parameter in the analysis of the LE- $\mu\text{SR}$  data. In addition microwave data on the same crystal is used to extrapolate the LE- $\mu\text{SR}$  values to  $T = 0$ .

Our average in-plane penetration depth  $\lambda_{ab} = \sqrt{\lambda_a\lambda_b} = 116.8(2.3)$  nm is in good agreement with the bulk  $\mu\text{SR}$  measurement in the vortex state on similar crystals [2]. In that case  $\lambda_{ab}$  was obtained by extrapolating the measurement of an effective  $\lambda$  in the vortex state down to zero magnetic field. Considering these are two very different types of measurement the agreement is remarkable and confirms that accurate values for  $\lambda$  can be obtained from conventional  $\mu\text{SR}$  in the vortex state provided the vortex lattice is well ordered. We find that the  $a$ - $b$  anisotropy is considerably less than found in early IR reflectivity measurements [16]. It is also less than reported for Gd doped Ortho-I phase ( $x = 6.995$ ,  $T_c = 89$  K) [17] but we anticipate that the anisotropy and  $\lambda$  are strong functions of doping since most of the charge carriers are being added to the chains in this doping region. The anisotropy from the current work is close to vortex state measurements using  $\mu\text{SR}$  and small-angle neutron scattering (SANS) on a large detwinned crystal of optimally doped  $\text{YBa}_2\text{Cu}_3\text{O}_{6.92}$  [18]. This is surprising since the effective  $a$ - $b$  penetration depth in this earlier generation of crystal appears to be considerably longer, possibly due to the increased role of scattering in this crystal. The current method should make it possible to study in much greater detail how  $\lambda$  and the anisotropy evolve as a func-

tion of doping in other exotic superconductors.

## SUMMARY AND CONCLUSION

In summary, we have used low-energy  $\mu$ SR to measure the magnetic field profiles in the Meissner state of a mosaic of detwinned single crystals of  $\text{YBa}_2\text{Cu}_3\text{O}_{6.92}$  at 8 K. Microwave resonator measurements were then used to extrapolate  $\lambda_{a,b}$  to  $T = 0$ . The in-plane anisotropy  $\lambda_a/\lambda_b = 1.20(1)$  is considerably less than reported from early IR studies and in ESR studies on Gd doped  $\text{YBa}_2\text{Cu}_3\text{O}_{6.995}$  but is close to that reported from early  $\mu$ SR and SANS experiments on a large detwinned crystal. The field profiles are exponential on the scale of  $\lambda$  but there are deviations close to the surface which are not yet understood. Finally, we have demonstrated that low-energy  $\mu$ SR can be used to study fundamental properties of crystals which are often smaller than the beam spot for low energy muons.

We would like to acknowledge helpful discussions with Jeff Sonier. This research was supported by the Paul Scherrer Institute, the Natural Sciences and Engineering Research Council of Canada and the Canadian Institute for Advanced Research. We would especially like to acknowledge H. P. Weber for his expert technical support.

---

\* masrur@phas.ubc.ca

- [1] A. J. Drew, F. L. Pratt, T. Lancaster, S. J. Blundell, P. J. Baker, R. H. Liu, G. Wu, X. H. Chen, I. Watanabe, V. K. Malik, A. Dubroka, K. W. Kim, M. Rössle, and C. Bernhard, *Phys. Rev. Lett.* **101**, 097010 (2008).
- [2] J. E. Sonier, S. A. Sabok-Sayr, F. D. Callaghan, C. V. Kaiser, V. Pacradouni, J. H. Brewer, S. L. Stubbs, W. N. Hardy, D. A. Bonn, R. Liang, and W. A. Atkinson, *Phys. Rev. B* **76**, 134518 (2007).
- [3] D. M. Broun, W. A. Huttema, P. J. Turner, S. Özcan, B. Morgan, R. Liang, W. N. Hardy, and D. A. Bonn, *Phys. Rev. Lett.* **99**, 237003 (2007).
- [4] M. Franz and A. P. Iyengar, *Phys. Rev. Lett.* **96**, 047007 (2006).
- [5] A. Serafin, J. D. Fletcher, S. Adachi, N. E. Hussey, and A. Carrington, *Phys. Rev. B* **82**, 140506 (2010).
- [6] T. J. Jackson, T. M. Riseman, E. M. Forgan, H. Glückler, T. Prokscha, E. Morenzoni, M. Pleines, C. Niedermayer, G. Schatz, H. Luetkens, and J. Litterst, *Phys. Rev. Lett.* **84**, 4958 (2000).
- [7] R. F. Kiefl, M. D. Hossain, B. M. Wojek, S. R. Dunsiger, G. D. Morris, T. Prokscha, Z. Salman, J. Baglo, D. A. Bonn, R. Liang, W. N. Hardy, A. Suter, and E. Morenzoni, *Phys. Rev. B* **81**, 180502 (2010).
- [8] E. Morenzoni, H. Glückler, T. Prokscha, H. P. Weber, E. M. Forgan, T. J. Jackson, H. Luetkens, C. Niedermayer, M. Pleines, M. Birke, A. Hofer, J. Litterst, T. Riseman, and G. Schatz, *Physica B: Condensed Matter* **289–290**, 653 (2000).
- [9] T. Prokscha, E. Morenzoni, K. Deiters, F. Foroughi, D. George, R. Kobler, A. Suter, and V. Vrankovic, *Nuclear Instruments and Methods in Physics Research Section A: Accelerators, Spectrometers, Detectors and Associated Equipment* **595**, 317 (2008).
- [10] K. Nagamine, S. Nagamiya, O. Hashimoto, N. Nishida, T. Yamazaki, and B. D. Patterson, *Hyperfine Interactions* **1**, 517 (1975).
- [11] W. Eckstein, *Computer Simulation of Ion-Solid Interactions* (Springer, Berlin, 1991).
- [12] E. Morenzoni, H. Glückler, T. Prokscha, R. Khasanov, H. Luetkens, M. Birke, E. M. Forgan, C. Niedermayer, and M. Pleines, *Nuclear Instruments and Methods in Physics Research Section B: Beam Interactions with Materials and Atoms* **192**, 254 (2002).
- [13] B. M. Wojek, Private communication.
- [14] M. Lindstrom, B. Wetton, and R. Kiefl, *Physics Procedia* **30**, 249 (2012).
- [15] W. N. Hardy, D. A. Bonn, D. C. Morgan, R. Liang, and K. Zhang, *Phys. Rev. Lett.* **70**, 3999 (1993).
- [16] D. N. Basov, R. Liang, D. A. Bonn, W. N. Hardy, B. Dabrowski, M. Quijada, D. B. Tanner, J. P. Rice, D. M. Ginsberg, and T. Timusk, *Phys. Rev. Lett.* **74**, 598 (1995).
- [17] T. Pereg-Barnea, P. J. Turner, R. Harris, G. K. Mullins, J. S. Bobowski, M. Raudsepp, R. Liang, D. A. Bonn, and W. N. Hardy, *Phys. Rev. B* **69**, 184513 (2004).
- [18] C. Ager, F. Y. Ogrin, S. L. Lee, C. M. Aegerter, S. Romer, H. Keller, I. M. Savić, S. H. Lloyd, S. J. Johnson, E. M. Forgan, T. Riseman, P. G. Kealey, S. Tajima, and A. Rykov, *Phys. Rev. B* **62**, 3528 (2000).